Extended Abstracts of the 2007 International Conference on Solid State Devices and Materials, Tsukuba, 2007, pp. 648-649

P-10-10

The Study of Organic Light Emitting Diode with a Doped Electron Transport Layer

Cheng-Chieh Hou*, Ruei-Shiang Shieh, Shui-Hsiang Su, Chung-Ming Wu and Meiso Yokoyama

Department of Electronic Engineering, I-Shou University, 1, Section 1, Hsueh-Cheng Rd., Ta-Hsu Hsiang, Kaohsiung County, Taiwan 840, R.O.C.
Phone: +886-7-6577257 *E-mail: d9302002@stmail.isu.edu.tw

1. Introduction

Organic light-emitting diodes (OLEDs) have been widely recognized as a technology for flat panel display (FPD) products today and for potential future use in the lighting industry [1-3]. Recently, doping techniques, which have been widely used in forming inorganic semiconductors, have been applied for forming organic p- and n-type materials [4]. Although efficient p-type doping is possible for a variety of organic materials, examples based on the n-type doping with high stability are rare [5]. A typical n-type doping electron transport layer (ETL) consists of a low work-function metal doped in an organic material. Co-evaporation of the materials, which is called the metal-doped technique, is commonly employed for preparing this ETL. In this study, we report the lithium (Li) doping to enhance electron injection in OLED. Additionally, this Li dopant will also improve the morphology of electron injection layer.

2. Experiments

Fig. 1 shows the structure of devices studied in this work, in which indium-tin oxide (ITO) on glass acts as an anode and theAl as a cathode. ITO with a thickness of 150 nm and a sheet resistance of 15Ω/sq was used as a substrate in the OLED. After the substrate was loaded into an evaporation system, organic layers were sequentially fabricated at a rate 1 ~ 2 Å/s onto substrates by thermal evaporation from resistively heated tantalum boats, at a base pressure of 2 ~ 5 x 10^{-6} Torr. The evaporation rate and thickness of the film was determined using an oscillating quartz thickness monitor (Sycon STM-100). The active area of the devices, defined by the overlap of the ITO and the Al electrodes, was 0.3×0.3 cm^2. All devices were encapsulated in a dry nitrogen glove box. The electron injection layer (ETL), we used Li as the dopant and tris(8-quinolinolato)aluminum Alq_3 as the host materials of the ETL. The metal doping concentration is 0%, 30%, 50%, 70% and 90 %, respectively. The luminance-current density (L-J) and the current density-voltage (J-V) characteristics were measured using a Topcon SR-1 luminance meter at room temperature and an HP4156A precision semiconductor parameter analyzer. X-ray photoelectron spectroscopy (XPS) measurements were performed in an ultrahigh vacuum system. The XPS spectroscopy, which consisted of a high power X-ray source operating at the Mg Kα line and an angle resolved electron energy analyzer, had an energy resolution of 1.2 eV. Atomic force microscopy (AFM) was used in an attempt to correlate these characteristics of the surface morphology.

3. Results and discussion

From an ITO/NPB (40 nm)/ Alq_3 (55 nm)/Li-doped Alq (5 nm)/Al (200 nm) device, having a Li to Alq ratio of Li/Alq=1 (Li doping 50% in Alq_3), green EL from the Alq layer was observed through the glass substrate when biased Al negative. Low voltage of 3.8 V is observed at 4.17 mA/cm^2 as seen in the current density–voltage characteristics of the device in Fig. 2. In contrast, a device without Li doping, ITO/ NPB (40 nm)/ Alq_3 (600 nm)/Al (200 nm), showed the voltage of 5.41V at 4.17 mA/cm^2 (shown in Fig. 2). Table I summarizes the performance of the devices at a drive current density of 104 mA/cm^2. These results clearly demonstrate that the Li doping to Alq at the cathode interface is effective in lowering the driving voltages and to balance the hole–electron injection, resulting in high device efficiencies. The Li was found to be one of the most efficient dopants, it would easily diffuse into the light-emitting layer (EML) and hence induce the metal ion quenching effect.

XPS studies show that the metal atoms are uniformly distributed through out the region of the sample which could be studied by photoelectron spectroscopy. N(1s) core level spectra of the nitrogen atom in the Alq_3 upon Li doping are shown in Fig. 3. The peak position of the N(1s) core level of pristine Alq_3 was 397.2 eV. The spectra are plotted without adjustment for changes in work function. Even at an early stage of Li doping, a new clear peak is observed on the low binding energy side of the original N(1s) peak. The peak position of the new peak by Li doping was 1.3 eV higher than N(1s) of pristine Alq_3. The other core levels, C(1s) and O(1s), did not show any significant change, even though the N(1s) was strongly affected by the Li doping. This suggests that donated electron is very localized on the N-sit, and that the changes of binding energy of the core levels induced by the chemical bond length change of Al-N are too small to affect the XPS spectra. Thus, the phenomenon can to enhance electron injection.

Figure 4 shows the AFM surface morphology of films deposited on glass substrates with the same thickness. The average surface roughnesses (root mean square average) are 4.4, 7.19, 2.74, and 1.15 nm for Alq_3 without or with annealing and Li doped Alq_3 without or with annealing, respectively (Fig. 4). Compare Fig. 4(a) with 4

(b), crystallization is evident in Alq_3 films after annealing at 200 °C for 30 min. However, by doping Alq_3 film with Li, the phenomenon of crystallization after annealing under the same condition is clearly suppressed. We expect therefore that the Li doped Alq_3 should improve device operational stability under thermal stress.

4. Conclusions

In conclusion, we have investigated that metal doping is an effective way to control electron injection from the cathode to the organic layer. The binding energy of N(1s) core level of Alq_3 was shifted by doping to lower binding energy, of 1.3 eV from the original peak for Li. the phenomenon can to enhance electron injection. We also find that Li doped Alq_3 layer has good morphological stability which is likely to reduce nonemissive dark spot growth.

References

[1] C. W. Tang and S. A. Vanslyke, Appl. Phys. Lett. **51** (1987) 913.

[2] C. W. Tang and S. A. Vanslyke, J. Appl. Phys. **65** (1989) 3610.

[3] R. Sheats, et al, Science, **273** (1996) 884.

[4] J. Huang, et al, Appl. Phys. Lett. **80** (2002) 139.

[5] S. T. Lee, et al, Appl. Phys. Lett. **75** (1999)1404.

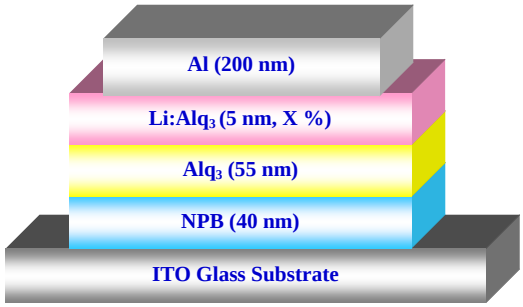

Fig. 1 Schematic diagram of the device configuration.

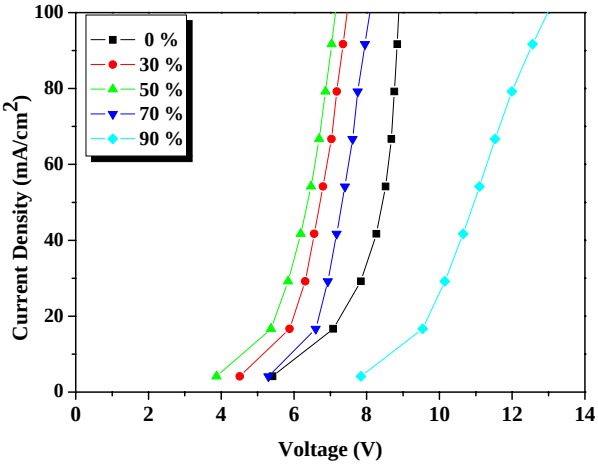

Fig.2 Comparison of current density versus voltage curves.

Table I. Characteristic performance of the OLEDs driven at 104 mA/cm^2

Device	Voltage (V)	Luminance (cd/m^2)	Efficiency (cd/A)
O%	8.9	117	0.1
30%	7.52	4960	4.67
50%	7.19	5450	5.25
70%	8.15	3715	3.44
90%	13.7	3090	2.5

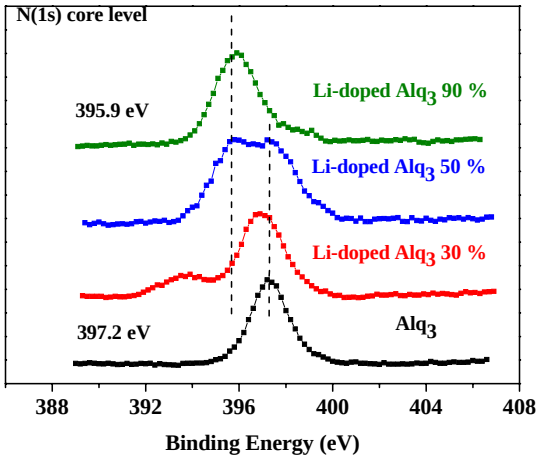

Fig. 3 N(1s) core level spectra of the nitrogen atom in the Alq_3 upon Li doping.

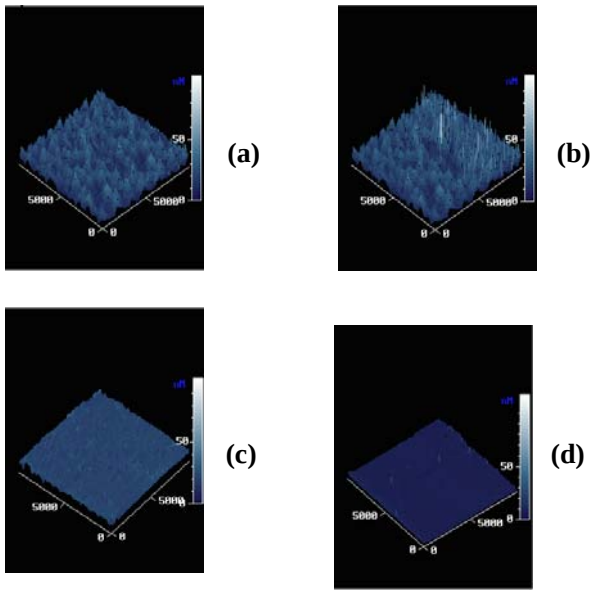

Fig. 4 Surface morphology of Alq_3 and Li doped Alq_3 by AMF. (a) Alq_3 without anneal, (b) Alq_3 with annealing, (c) Li doped Alq_3 without annealing, and (d) Li doped Alq_3 with annealing.